

# EVALUATING THE LABORATORY PERFORMANCE OF CIRCULAR MATERIALS AS BITUMEN SUBSTITUTE



GEBR.  
VAN DER LEE

Paving the way to a sustainable  
asphalt construction industry

CHRIS VAN DE POL  
17-08-2021

UNIVERSITY  
OF TWENTE.

# Evaluating the Laboratory Performance of Circular Materials as Bitumen Substitute

**C.R. (Chris) van de Pol**

MSc. Construction Management & Engineering

*University of Twente*

*Gebr. Van der Lee*

August 17, 2021

## **Abstract**

With the effects of climate change becoming more visible, governments are progressively taking actions to reduce environmental impact. This in turn incentivizes the asphalt construction industry to adopt more environmentally sustainable practices. One of these practices is replacing the fossil bitumen binder in asphalt mixtures by circular materials, which could reduce the environmental significantly by lowering the need for bitumen and improving the performance of the final product. However, most studies on this subject substituted only a small percentage of the binder by the circular material, after which the modified binder was compared to the neat bitumen, which due to different stiffness cannot be used for the same application. This paper fills this gap by comparing the performance of five circular materials as bitumen substitute for varying weight ratios of the binder on rutting and fatigue resistance, required mixing and compaction temperatures and linear viscoelastic behaviour on an equi-stiffness level by using multiple penetration grade bitumen. The results showed similar to improved performance for binders containing up to 51.69% of circular materials. It can be concluded that high shares of certain circular materials can be added to the binder without significantly compromising or even improving the binder performance while reducing the environmental impact of the industry.

**Keywords:** Asphalt, bitumen, binder, substitute, environmental impact, circular, fatigue

## **1 Introduction**

In 2016, the Paris Climate Agreement was adopted to limit global warming well below 2 °C and preferably 1.5 °C compared to pre-industrial levels [1]. Global warming was estimated at 1 °C in 2018, whereas the IPCC expects to reach 1.5 °C between 2030 and 2052 [2]. Though climate change affects all individuals, the responsibility is mostly placed at governments and companies, in turn also affecting the asphalt construction industry [3, 4, 5, 6]. The main Dutch road agency Rijkswaterstaat uses the CO<sub>2</sub> performance ladder and Environmental Cost Indicator (ECI, Dutch: MKI) to objectively measure the sustainability of offers in tenders.

Environmental sustainability can play a major role in public tenders, sometimes being able to lower the actual bid by 40% in the selection process [7]. The asphalt construction industry can implement several measures to be more environmentally sustainable. One is to increase the amount of reclaimed asphalt in the production of new asphalt mixtures, which is very beneficial to circularity and widely applied. However, as long as the demand for new asphalt mixture is greater than the supply of reclaimed asphalt, there will be a limit to this amount. In 2017, the maximum theoretical recycling rate was only 56% for the Netherlands, assuming all reclaimed asphalt to be used in the production of new asphalt mixtures [8]. Another is to use polymer modified bitumen as a binder in asphalt mixtures. Due to the polymer modification, the mechanical properties of asphalt pavements can be improved, thus allowing thinner layers and/or increased life expectancy. However, the polymer modifications themselves have a significantly high impact on the environment [9]. Much interest is put in lowering the production temperature of asphalt mixtures, which is mainly dependent on the binder. Measures such as in-situ recycling, epoxy modification, electrification and improved asphalt plant designs are less well established, but growing in interest. In this paper, the focus will be placed on evaluating the laboratory performance of binders being composed of circular materials as bitumen substitute in order to reduce the environmental impact and increase performance. In this study, circular materials are defined as being waste materials and/or bio-based materials.

## **1.1 Problem definition**

Though the use of circular materials as bitumen substitute is not as mature as asphalt recycling and production temperature reduction practices, many studies have been performed on this subject [10, 11]. Most studies evaluate the effect of these bitumen substitutes by adding an arbitrary amount of material to bitumen, after which the performance of the modified binder is compared to the same neat bitumen. The results of these studies are generally an increase in high temperature performance and a decrease in low temperature performance or vice versa, which is then attributed solely to the material. However, the stiffening or softening effect of the materials on the binder is often ignored when analyzing the performance. Furthermore, due to their different stiffness, it is unlikely that both the neat bitumen and modified binder can be used for the same asphalt mixture and application. This research will fill in this gap by evaluating the performance of circular materials as a bitumen substitute on an equi-stiffness level.

## **1.2 Research objective**

The goal of this research is to evaluate the laboratory performance of various circular materials as bitumen substitute by comparing them on an equi-stiffness level. To fulfill this objective, experiments are conducted on how the various circular materials affect the stiffness of the binder when mixed with bitumen. Subsequently, the laboratory performance

is compared between the neat bitumen and the binders composed of varying weight ratios of circular materials on an equi-stiffness level with respect to rutting and fatigue resistance, required mixing and compaction temperatures and linear viscoelastic behaviour. The results of this study are the first step towards the direct use of the circular materials in asphalt mixtures for performance testing and can function as the basis for a deeper study on the development of a 100% circular binder by combining multiple circular materials.

### 1.3 Outline

The outline of this paper is divided in 5 main sections. It starts by introducing the problem statement and research objective in section 1. Section 2 introduces the materials and methods considered in this study. Therein, the experimental procedure is presented, followed by a description of the various methods that were used in this research. In section 3, the results are presented and discussed. Section 4 presents the conclusions drawn from this study, followed by recommendations on the continuation of this research in section 5.

## 2 Materials and methods

In this research, five circular materials were considered, listed as A, B, C, D and E. Furthermore, 160/220, 100/150, 70/100, 40/60 and 20/30 penetration grade bitumen were used.

### 2.1 Experimental procedure

The experimental procedure was divided in two phases, as visualized in figure 1.

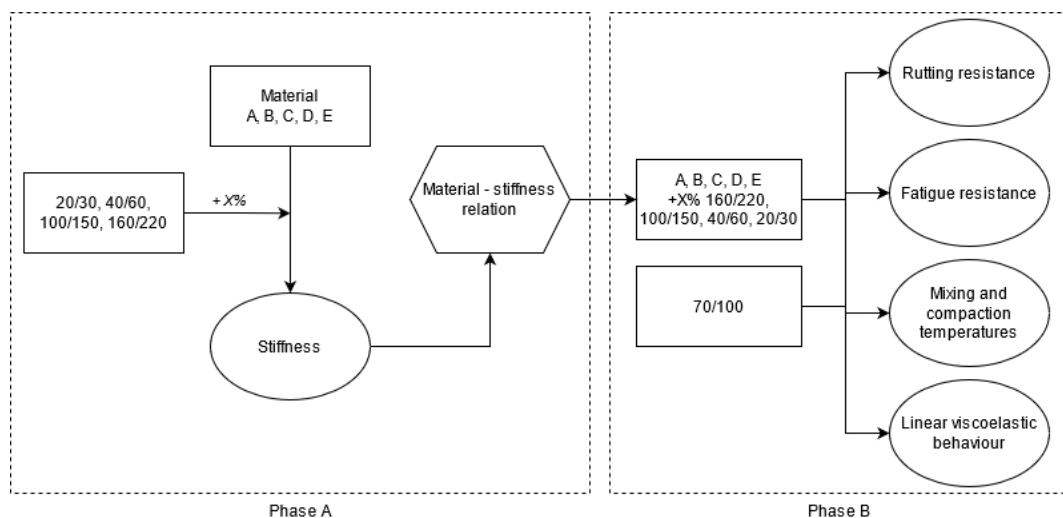


Figure 1: Experimental procedure

In phase A, the aim was to determine the influence of each circular material on the stiffness of the binder when mixed with a particular bitumen for a specific weight ratio, creating

a relation between the material and the stiffness of the binder. In phase B, the circular materials were blended using the determined weight ratios with the various bitumen, in order to create binders with similar stiffness to a neat 70/100 bitumen. The 70/100 bitumen stiffness was chosen as equi-stiffness level due to 70/100 being a commonly used penetration grade bitumen in Dutch asphalt mixtures. For the binders composed of circular materials, the laboratory performance was determined as well as for the neat 70/100 bitumen. In the following sections, further details will be given on the methods executed and tests performed.

## **2.2 Creating binder blends**

In phases A and B, minimal binder blends of 100g and 300g were created respectively due to a limited availability of materials. The mixing temperature was set at 130 °C for all blends, whereas some circular materials in binders were observed to be susceptible to higher temperatures. In preparing the blends, the bitumen was heated to 130 °C for 5 hours. The circular materials were heated to either 130 °C or the maximum allowed temperature of the material, whichever was lowest, for the same duration. After weighing, the blends were manually homogenized and reheated to 130 °C for 1.5 hours. Finally, the blends were homogenized using a high shear mixer at 4500 rpm for 10 minutes in phase A. In phase B, only 3000 rpm were used for 20 minutes, to limit the heat induced by the high shear mixer at greater volumes.

## **2.3 Stiffness**

To determine the stiffness of the blends in phase A, a frequency sweep was conducted at the temperature of 20 °C using a Dynamic Shear Rheometer (DSR). The goal was to simulate the same stiffness as done in the 4-pt bending test on asphalt mixtures, which measures the stiffness at 8 Hz at 20 °C. For the oscillatory DSR test, this translates in a frequency of around 1.27 Hz [12]. In this research, the stiffness was measured as the complex modulus  $G^*$  at 20 °C at a frequency of 1.26 Hz using the PP8 geometry with a 2mm gap at a strain level of 0.05%.

## **2.4 Rutting resistance and elastic recovery**

In phase B, the rutting resistance including the elastic recovery was determined for each binder using the Multiple Stress Creep Recovery (MSCR) method. This method is suitable for both neat and modified binders, since it reflects elastic behaviour better [13, 14]. For the MSCR test, the PP25 geometry used with a 1mm gap. During the MSCR test, the DSR repeatedly applies 1s of shear stress on the specimen, after which it is allowed to recover for 9s while measuring the resulting shear strain, which was repeated for multiple cycles. In this research, 20 cycles using a shear stress of 0.1 kPa were used followed by 10 cycles using 3.2 kPa at 60 °C. The first 10 cycles of 0.1 kPa were not used for analysis, but were meant to achieve a steady-state condition was recommended by the latest standards [14].

The output of the MSCR test is the non-recoverable creep compliance  $J_{nr}$  and the recovery percentage  $R$ .  $J_{nr}$  represents the resistance against deformation and  $R$  the presence of elastic response [14]. In some cases,  $R$  can show a negative value when the shear strain increases after the 1s of loading, which can be caused by the DSR removing the shear stress too slow or the inertia of the geometry. Some standards prescribe to report 0 for  $R$  when the calculated value is negative [14]. In this research,  $R$  is calculated using the maximum strain during the whole creep recovery cycle, instead of the strain at the end of the 1s of loading. An optimal binder shows a low non-recoverable creep compliance  $J_{nr}$  and a high recovery  $R$ . The stress sensitivity of  $J_{nr}$  and  $R$  between 0.1 and 3.2 kPa is calculated as the percentage difference resulting in the  $J_{nr-diff}$  and  $R_{diff}$ , which should be low for an optimal binder [15].

## 2.5 Fatigue resistance

To determine the fatigue resistance of each binder, both the Linear Amplitude Sweep (LAS) and Time Sweep (TS) methods were employed. Both are able to determine the fatigue resistance in the number of cycles to failure for a specific strain level, similar to the 4-pt bending fatigue test. The LAS method is relatively quick compared to the TS method and predicts the cycles to failure using a Visco-Elastic Continuum Damage (VECD) analysis. For both methods, the cycles to failure were calculated using both the  $G^R - N_f$  and  $W_{sum}^R - SE$  frameworks [16, 17]. The main difference between the two frameworks is their failure definition which defines at which cycle the binder has failed. The  $G^R - N_f$  framework defines binder failure at the cycle where  $C \times N$  yields maximum.  $N$  is the cycle number and  $C$  the complex modulus  $G^*$  measured at that cycle divided by the initial stiffness of the binder. The  $W_{sum}^R - SE$  framework defines binder failure at the cycle where  $C^2 \times N \times (1 - C)$  yields maximum, which is said to perform better when comparing aged to neat binders [17]. In this research, the LAS and TS were performed for the same conditions at a frequency of 10 Hz at 10 °C using the PP8 geometry with 2mm gap. The temperature was chosen due to being the average spring temperature of the Netherlands, where spring is considered to pose the most critical conditions on pavement deflection [18]. To achieve a more accurate fit of the VECD model, TS were incorporated for each binder at a strain level of 5%, which were also used to validate the VECD models.

## 2.6 Mixing and compaction temperatures

In order to determine the required mixing and compaction temperatures of the binders in phase B, the Equi-Viscous Temperature (EVT) method was used which is common method to determine recommended mixing and compaction temperatures for bitumen. Using the EVT, the temperature at which the viscosity is equal to 0.17 Pa s and 0.28 Pa s is determined for mixing and compaction respectively [19]. To allow an accurate measurement of modified binders which can show non-Newtonian behaviour at high temperatures such as shear thinning, the viscosity is taken at a shear rate of 500 1/s. For the viscosity measurements, the

DSR was used equipped with the PP25 geometry at a 1mm gap. The rotational viscosity was determined at 135 °C and 165 °C at 185 1/s and 300 1/s, which was linearly extrapolated to 500 1/s. By interpolating between the log temperature and log viscosity, the EVT was determined for both mixing and compaction.

## 2.7 Linear viscoelastic behaviour

The linear viscoelastic behavior of the binders in phase B is represented by their black diagram, temperature shift factors and master curves. In order to construct these, frequency sweeps were performed at temperatures ranging from -10 °C to 20 °C and 30 °C to 70 °C using the PP8 and PP25 geometries on the DSR respectively at 0.05% strain. By plotting the complex modulus  $G^*$  against the phase angle  $\delta$ , the black diagram is obtained. A continuous black diagram indicates that the Time-Temperature Superposition Principle holds for the binder, thus enabling the formation of a master curve by applying temperature shift factors [20]. Furthermore, the black diagram is able to show elastomeric behaviour when the phase angle decreases at a low stiffnesses. Using the Equivalent Slope Method (ESM), the isothermals from the frequency sweeps were shifted along the frequency axis to form a smooth curve [21]. On these predicted shift factors, the William-Landel-Ferry (WLF) equation was fitted, which determined the temperature shift factors for each temperature with respect to the reference temperature, which was set at 20 °C. By plotting these shift factors over a certain temperature range, the dependency of the binder stiffness to temperature can be visualized [22]. It was hypothesized that a decreased temperature dependency would result in increased mixing and compacting temperatures and decreased rutting resistance and vice versa. The master curves were constructed using the WLF temperature shift factors. For the complex modulus  $G^*$  master curve, it was hypothesized that a lower stiffness at low frequencies would result in increased fatigue resistance. Both hypothesis are tested on the binders and neat 70/100 bitumen in phase B.

## 2.8 Material - stiffness relation

To determine how each circular material affects the stiffness of the binder when mixed with bitumen, a relation needs to be established. This relation will enable the creation of equi-stiffness binders. In equation 1, this relation is shown, inspired by the log-pen rule and the work of Varanda et al [23].

$$\log(G^*_{mix}) = \sum_i X_i \cdot \log(G^*_i) + \sum_i \sum_{j(j<i)} \beta_{ij} X_i X_j \quad (1)$$

$G^*_{mix}$  is the stiffness of the blended binder,  $X_i$  the weight ratio of the specific material in the blend and  $G^*_i$  the stiffness of the material. Since some combinations of materials can interact differently, the interaction coefficient  $\beta_{ij}$  is introduced. It was determined using a regression analysis on the binder stiffness measured at 20 °C at 1.26 Hz in phase A and only included

if statistically significant ( $p \leq 0.05$ ). If the material itself could not be directly measured using the DSR,  $G^*_i$  was also determined via the regression analysis.

### 3 Results

#### 3.1 Phase A

Multiple blends of different combinations of circular materials and bitumen were made in phase A to establish the material-stiffness relation. For each blend, three replicates were made for the frequency sweep at 20 °C. In table 1, the parameters of equation 1 are given along with the goodness-of-fit  $R^2$  of the regression analysis.

Material	Log $G^*_i$ (Pa)	$\beta_{ij}$	$R^2$
A	5.8902	1.4093	0.9916
B	7.7598	-	0.9973
C	11.8002	-11.9099	0.9155
D	22.2911	-27.1763	0.9985
E	2.8424	-0.4439	0.9959

Table 1: Regression analysis results

Overall, equation 1 provided a workable fit for all circular materials considered when mixed with bitumen for phase B. The log  $G^*$  of material A determined via the regression analysis is similar to the 70/100 bitumen, which is around 5.88 Pa. However, when blended with bitumen, the interaction coefficient increases the stiffness of the blend significantly. During the experiments, it was observed that blends containing more than 50% of material A could not be homogenized, since all bitumen was absorbed by the material. The stiffness of material B was determined to be significantly higher than that of the 70/100 bitumen, but had no statistically significant interaction coefficient when mixed with bitumen. It was observed that blends consisting of over 30% of material B showed a higher variability in stiffness, indicating that those binders were either not homogeneous or unstable. The regression analysis on the blends containing material C resulted in the lowest  $R^2$  compared to the other materials, which could indicate that equation 1 does not hold for material C. For one bitumen grade, it was observed that material C could both stiffen and soften the binder, depending on the ratio. The stiffness of material C was determined via the regression analysis, since the directly measured stiffness of material C resulted in an even worse fit. For blends containing over 60-70% of material C by weight, a great variability in stiffness was observed. Material D was observed to soften the binder in all experiments. Since the stiffness of material D could not be measured using the DSR, the stiffness was determined by the regression analysis, which resulted in a significantly higher stiffness than that of the 70/100 bitumen. This is compensated by the high negative interaction coefficient and thus

provided a good fit. The stiffness of material E could be determined directly, and combined with the interaction coefficient provided a good fit in the regression analysis. Due to the low stiffness of material E, it showed a softening effect on the binder, helped by the small negative interaction coefficient. The high goodness-of-fit of the regression analysis using relation 1 on the circular materials in binder blends indicate relation 1 to perform very well in determining the stiffness of binder blends. However, since the relation predicts the  $\log G^*$ , minimal deviations from the fit can result in high deviations of the stiffness  $G^*$ . The relatively low goodness-of-fit for material C and the inability to include the measured stiffness in the regression analysis without worsening the fit indicates that relation 1 does not capture all interactions between some materials and bitumen. Furthermore, the high stiffness as determined by the regression analysis for material D does not correspond with the soft appearance of this material, though the regression analysis did result in a good fit.

Using the parameters from table 1 in relation 1, the weight ratio was determined for each combination of bitumen and material, in order to obtain a binder with similar stiffness to the 70/100 bitumen being  $\log 5.88$  Pa, as shown in table 2.

Material	160/220	100/150	40/60	20/30
A	46.31%	11.95%	-	-
B	25.90%	8.27%	-	-
C	54.88%*	51.69%	44.70%*	-
D	91.00%*	90.61%*	5.56%	13.69%
E	-	-	13.73%	24.87%

\* not considered

Table 2: Material weight ratios phase B

Table 2 presents some combinations of bitumen and materials which were not considered in phase B. For material D, no blends were made in phase A containing over 90% of material D, thus, it is unknown if relation 1 holds for these high ratios of material D. For material C, no blends were made in phase A combined with 40/60 bitumen. The blends containing material C in phase A combined with 160/220 bitumen all resulted in a lower stiffness than that of the 70/100 bitumen, which could not be accurately predicted by relation 1 and thus resulted in a lower  $R^2$ , as showed in table 1. For all other combinations, blends were created to be used for laboratory performance testing in phase B.

### 3.2 Phase B

In phase B, 9 binders and a neat 70/100 bitumen were considered. To validate that the stiffness of all binders in phase B was comparable to that of the 70/100 bitumen, the stiffness was measured again at 1.26 Hz at 20 °C. In figure 2, the average stiffness of two replicates is showed for each binder, along with the standard deviation. The yellow dashed line represents

the stiffness of the 70/100 bitumen as measured in phase A, to which all binders were designed as equi-stiffness level.

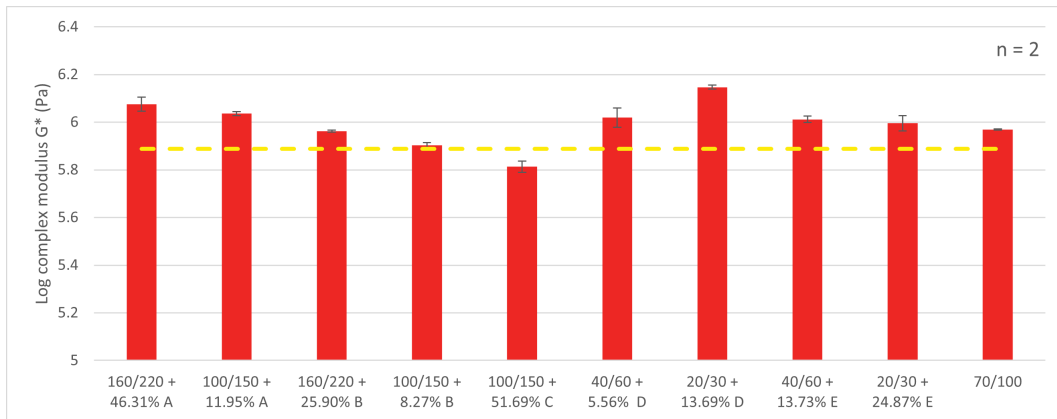
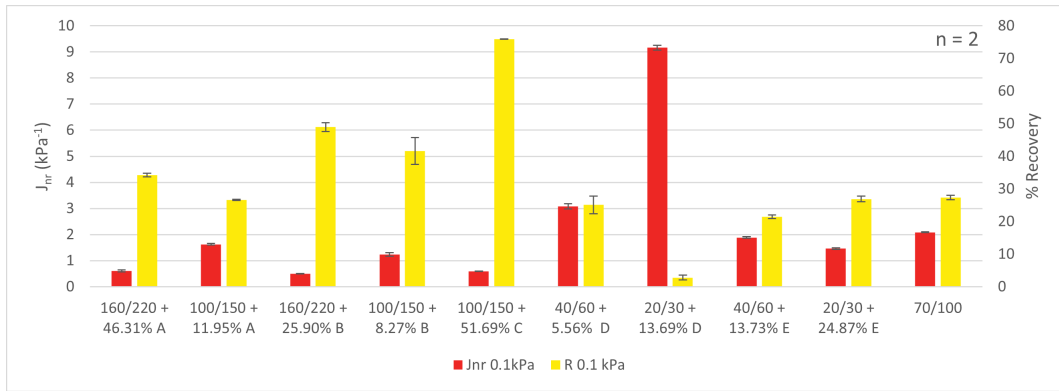


Figure 2: Phase B binder stiffness

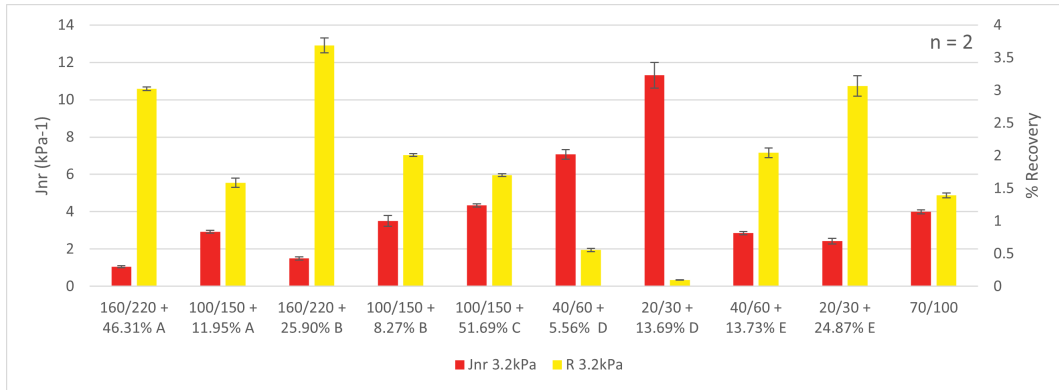
It can be observed that the 70/100 bitumen was more stiff in phase B compared to phase A, which could be explained by more significant aging due to the longer mixing duration in phase B. However, no conclusions can be drawn on the individual susceptibility to aging of the individual binders, since their difference in stiffness can also be caused by inaccurate weighing of the blends and relation 1 being not fully accurate. Though the stiffness of all binders was not exactly equal, it was thought that the differences were small enough such that this would not have a great impact on comparing the laboratory performance between the binders.

### 3.2.1 Rutting resistance and elastic recovery

For all binders and the neat 70/100 bitumen in phase B, the MSCR test was performed using two replicates determining the non-recoverable creep compliance  $J_{nr}$  and recovery percentage  $R$ . In figure 3a and 3b, the average  $J_{nr}$  and  $R$  are shown for 0.1 kPa and 3.2 kPa along with the standard deviation respectively. Table 3 shows the average  $J_{nr-diff}$  and  $R_{diff}$  along with the standard deviation of the two replicates, describing the stress-sensitivity of the binders based on the  $J_{nr}$  and  $R$ .



(a) 0.1 kPa



(b) 3.2 kPa

Figure 3:  $J_{nr}$  and  $R$  results from MSCR test for (a) 0.1 kPa and (b) 3.2 kPa

Blend	$J_{nr\_diff}$		$R_{diff}$	
	Average	St_dev	Average	St_dev
160/220 + 46.31% A	73.06%	0.87%	91.15%	0.06%
100/150 + 11.95% A	79.92%	1.15%	94.04%	0.30%
160/220 + 25.90% B	196.87%	10.35%	92.45%	0.45%
100/150 + 8.27% B	186.08%	38.08%	95.12%	0.53%
100/150 + 51.69% C	626.29%	16.24%	97.76%	0.03%
40/60 + 5.56% D	129.90%	15.30%	97.77%	0.15%
20/30 + 13.69% D	23.29%	6.35%	96.21%	1.03%
40/60 + 13.73% E	50.94%	2.42%	90.43%	0.60%
20/30 + 24.87% E	65.54%	6.55%	88.57%	0.94%
70/100	91.23%	3.17%	94.89%	0.27%

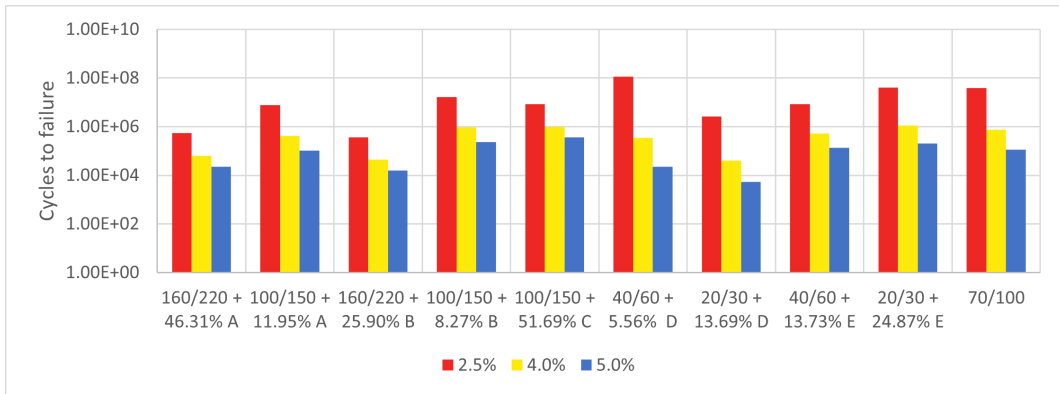
Table 3:  $J_{nr\_diff}$  and  $R_{diff}$  results from MSCR test for (a) 0.1 kPa and (b) 3.2 kPa

From figure 3, it can be seen that the results of the MSCR test for all binders were quite diverse. For both materials A and B, it was observed that they were able to decrease the  $J_{nr}$

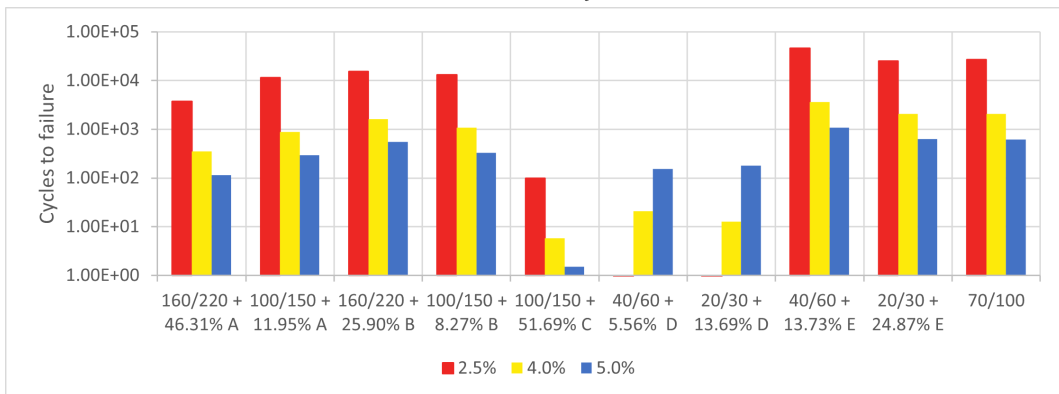
for both stress levels, where material A performed slightly better than material B at high stress levels, which was the opposite at low stress levels. Both were able to increase the recovery percentage  $R$  compared to the neat 70/100 bitumen, in which material B performed better at both stress levels. Material C showed the highest  $R$  accompanied by a low  $J_{nr}$  at low stress levels. However, at high stress levels, this effect was greatly diminished, though still observed. Material D increased the  $J_{nr}$  and decreased  $R$  for both stress levels, resulting in worse rutting resistance. Material E seemed to slightly lower the  $J_{nr}$  and increase  $R$  for both stress levels compared to the neat 70/100 bitumen. Table 3 confirms the high stress sensitivity of material C. It also shows the binders containing material B to have a high stress sensitivity, as well as the blend containing 5.56% material D. For the recovery percentage, there was no significant difference on the stress sensitivity between the binders, besides material E seemingly lowering it to a small extent. The MSCR tests show that stiffening materials increase rutting resistance by decreasing the  $J_{nr}$ . Softening materials showed to be able to either increase or decrease rutting resistance, depending on the material. Elastic recovery of the binder can be both enhanced as worsened significantly by certain materials. The rutting resistance of some binders for certain materials is very stress-sensitive as showed by the high  $J_{nr\_diff}$ . In some North-American standards, it is specified that the  $J_{nr\_diff}$  of a binder should not exceed 75% [14]. A fair amount of binders including the 70/100 bitumen exceed this threshold. However, it is unknown how this increased stress-sensitivity influences the performance of asphalt mixtures.

### 3.2.2 Fatigue resistance

For all binders including the neat 70/100 bitumen, the number of cycles to failure  $N_f$  was calculated for 2.5%, 4% and 5% strain using the  $G^R - N_f$  and  $W_{sum}^R - SE$  VECD frameworks. In figure 4, the results of both VECD frameworks are presented. In order to validate the results of the VECD frameworks, its results were plotted against the measured  $N_f$  from the Time Sweep (TS) at 5% strain. In figure 5, the  $N_f$  of both VECD frameworks are set out against average  $N_f$  of two replicates of the TS at 5% strain including the standard deviation. The orange line shows the line of equality, on which the points should lie if the VECD frameworks fully correspond with the TS results. Note that the two TS at 5% strain used in this validation were also used in the VECD framework.

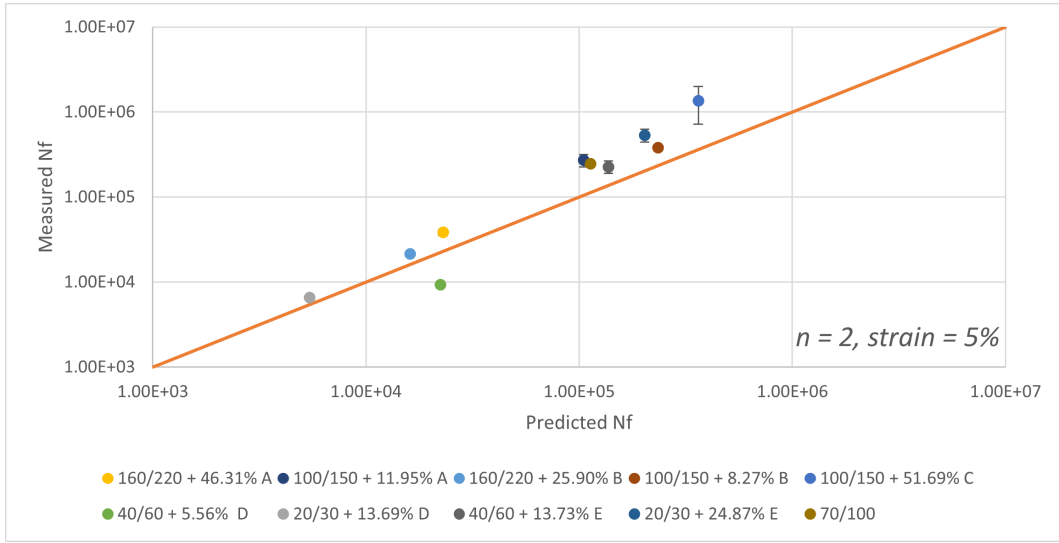


(a)  $G^R - N_f$

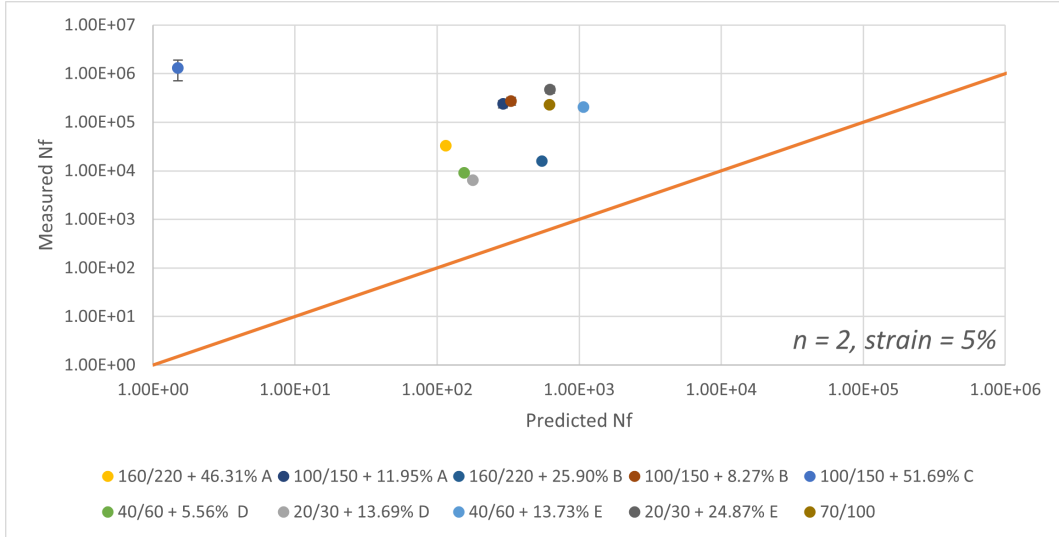


(b)  $W_{sum}^R - SE$

Figure 4: VECD fatigue resistance



(a)  $G^R - N_f$



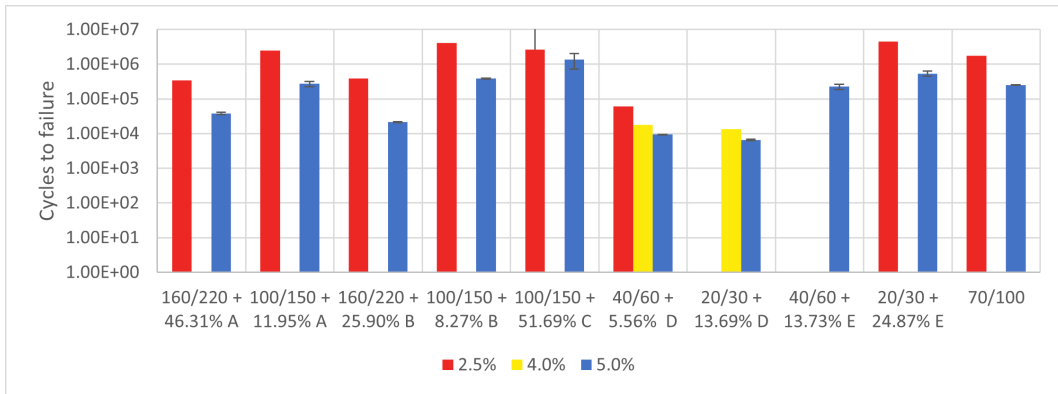
(b)  $W_{sum}^R - SE$

Figure 5: Validation of VECD frameworks at 5% strain

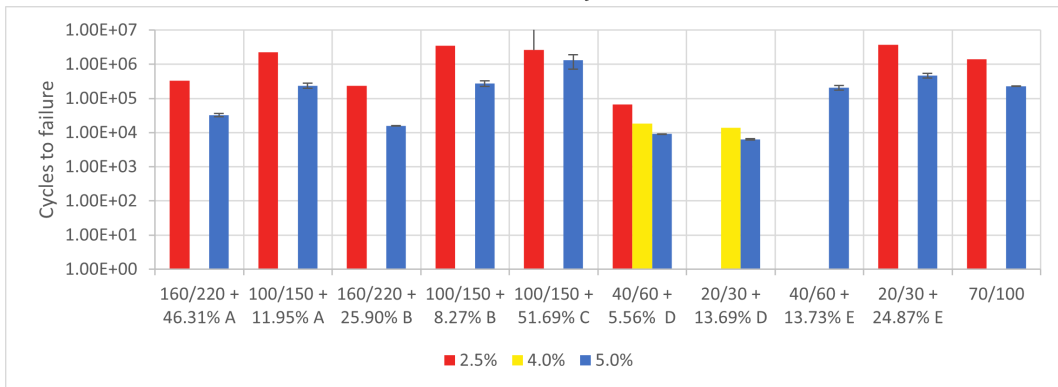
Figure 4 shows a significant difference between the predicted  $N_f$  of both frameworks, in the order of magnitude of  $1.00E + 05$ . Due to both frameworks using different failure definitions, some difference was expected, though not of this magnitude. In figure 4b, it was observed that the binders containing material D showed a higher  $N_f$  for higher strain levels, which was the opposite for all other binders. From figure 5, it can be observed that neither of the frameworks was able to fully accurately predict the  $N_f$  at 5% strain. For the  $G^R - N_f$  framework, a  $R^2$  of 0.934 was obtained, while for the  $W_{sum}^R - SE$  a negative  $R^2$  of -0.234 was determined. The high  $R^2$  of the  $G^R - N_f$  framework indicates that there was good correspondence between the VECD and TS results, while the negative  $R^2$  of the  $W_{sum}^R - SE$  indicates no correspondence

between the VECD and TS results. The bad performance of the  $W_{sum}^R - SE$  framework was unexpected, due to this framework being more complex than the  $G^R - N_f$  framework.

Due to the need to include the TS at 5% strain in the VECD framework to obtain correspondence for at least the  $G^R - N_f$  framework, it was decided to perform TS at 2.5% and 4% strain for the binders for further validation, even though TS at these low strain levels take be extremely long to perform. In figure 6, the measured  $N_f$  for all time sweeps performed on the binders are presented. For the 5% strain level, the average of two replicates are given including the standard deviation. For the 4% and 2.5% strain level, the TS was only performed at a selection of the binders using one replicate due to the long duration. For the 100/150 + 51.69% C binder, the TS at 2.5% strain was cancelled before the binder failed, thus the actual  $N_f$  is expected to be higher. In figure 7, the average TS results of figure 6 are plotted against the VECD results for both the  $G^R - N_f$  and  $W_{sum}^R - SE$  frameworks categorized per binder. The orange line again represents the line of equality.

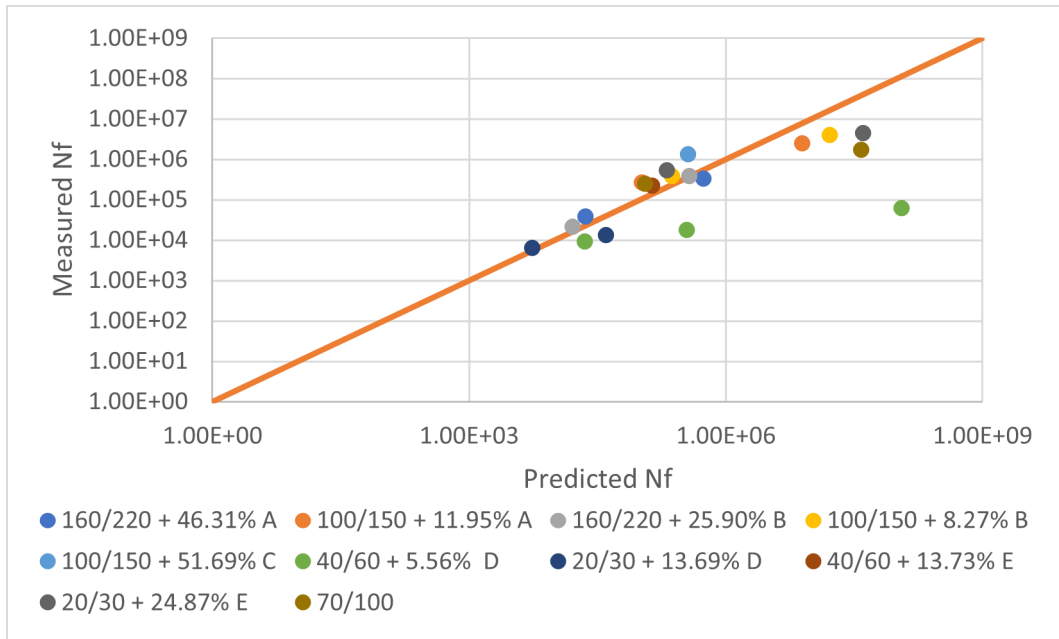


(a)  $G^R - N_f$

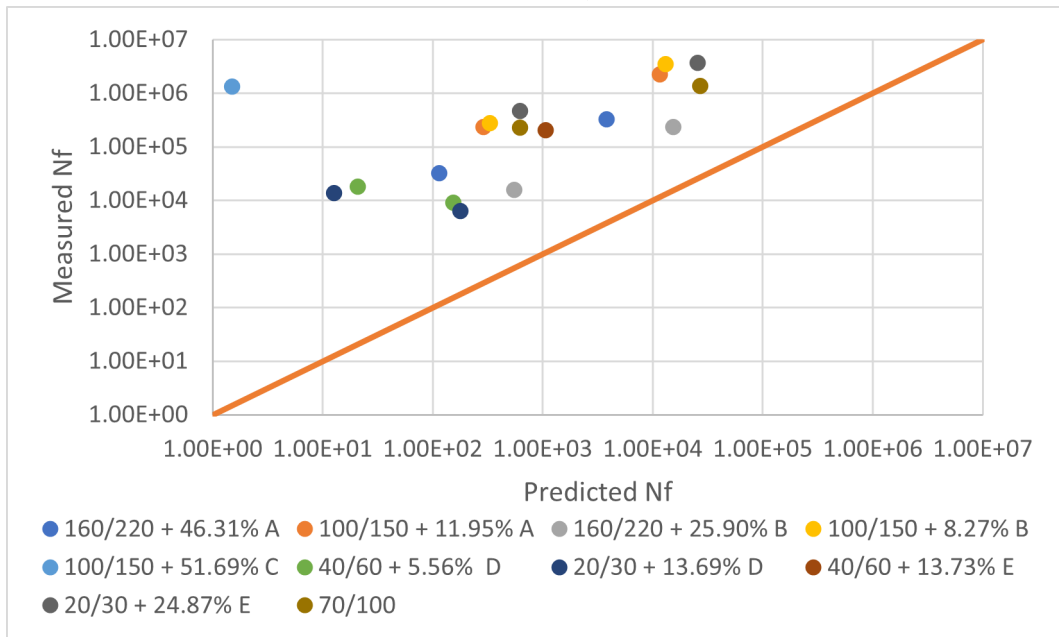


(b)  $W_{sum}^R - SE$

Figure 6: Time sweep fatigue resistance



(a)  $G^R - N_f$



(b)  $W_{sum}^R - SE$

Figure 7: Validation of VECD frameworks at varying strain levels

Figure 6 shows that there is some difference between the measured  $N_f$  for the different failure definitions of the  $G^R - N_f$  and  $W_{sum}^R - SE$  frameworks based on the TS, but far less than was observed in figure 4 between the VECD frameworks. Furthermore, all binders showed increased fatigue resistance at lower strain levels. From figure 7a, it can be observed that the  $G^R - N_f$  framework performs worse in accurately predicting the  $N_f$  at low strain levels (increased  $N_f$ ). Though the  $W_{sum}^R - SE$  predicted  $N_f$  in figure 7b are still off the line of

equality, the results at lower strain levels are evenly off at low strain levels. The  $R^2$  of the predicted and measured  $N_f$  at varying strain levels of the  $G^R - N_f$  framework was determined at 0.76, which is quite lower than the  $R^2$  when only validating using the 5% strain level. For the  $W_{sum}^R - SE$ , an  $R^2$  of 0.618 was achieved, significantly higher than when only validating using 5% strain.

The low  $R^2$  of both the  $G^R - N_f$  and  $W_{sum}^R - SE$  frameworks compared to the TS results could indicate the VECD frameworks to be less suitable for binders containing circular materials. Another explanation could be that both frameworks are very sensitive to the increase of strain during the LAS, which was not fully linear in this research because of the DSR being torque-controlled. The increased  $R^2$  of the  $W_{sum}^R - SE$  when validating using TS at varying strain levels could indicate the  $W_{sum}^R - SE$  framework to perform better in determining the  $N_f$  at low strain levels, whereas this is the opposite for the  $G^R - N_f$  framework.

Due to both VECD models being unable to accurately predict the fatigue resistance of the binders, the TS results as presented in figure 6 were analyzed. Materials A and B both showed similar to increased fatigue resistance compared to the 70/100 bitumen at low concentrations for all strain levels. At increased concentrations, their fatigue resistance was worse. Material C showed the highest fatigue resistance at 5% strain of all binders. Material D performed worse compared to the 70/100 bitumen for all strain levels. For material E, similar to increased fatigue resistance was observed at all strain levels compared to the 70/100 bitumen, which increased with the increasing concentration of material E in the binder.

### 3.2.3 Mixing and compaction temperatures

For all binders including the neat 70/100 bitumen, the mixing and compaction temperatures were determined using the procedure as described in section 2.6. In figure 8, the average mixing and compaction temperatures are showed including the standard deviation of two replicates for each binder.

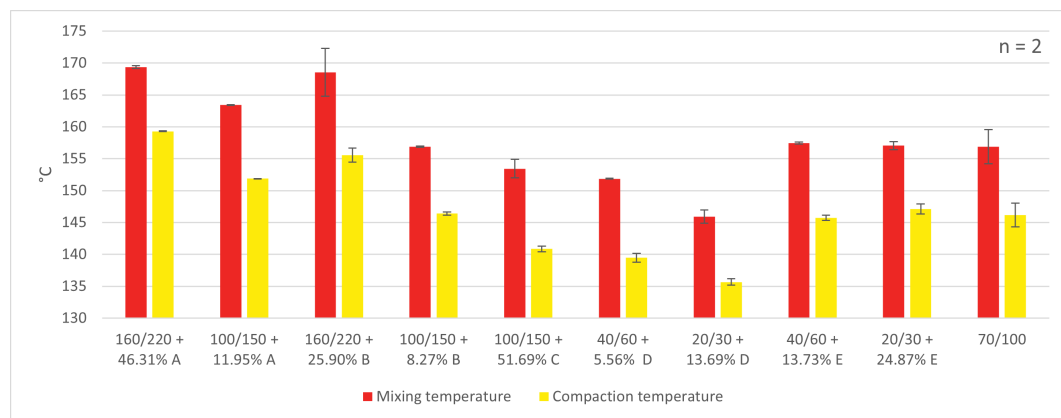


Figure 8: Mixing and compaction temperatures

In section 2.2, it was stated that some binders were observed to be susceptible to temperatures above 130 °C. In determining the mixing and compaction temperatures, the binder viscosity was measured at 135 °C and 165 °C, as described in section 2.6. It can therefore be expected that some binders were negatively affected during the viscosity measurements, which could have influenced the results. The methodology used in determining the mixing and compaction temperatures showed good reproducibility due to the overall low standard deviation between the replicates. Furthermore, the mixing and compaction temperatures for the neat 70/100 bitumen corresponded well to the mixing and compaction temperatures as used in practice. However, all binders required higher mixing and compaction temperatures than the 130 °C which was used in creating the binders due to some circular materials being susceptible to higher temperatures. This could result in some binders being negatively impacted when the required mixing and compaction temperatures are used, or in insufficient mixing and compaction when the temperature is limited to 130 °C without taking additional measures. From figure 8, it can be seen that the binder composed of 20/30 + 13.69% D required the lowest mixing and compaction temperatures, whereas the 160/220 + 46.31% A binder required the highest. Though some difference was observed in the temperature difference between mixing and compaction temperatures for the binders, it was marginal. Both material A and B required higher mixing and compaction temperatures as their share in the binder increased. For material D, the opposite was observed. Material E did not affect the mixing and compaction temperatures significantly when compared to the neat 70/100 bitumen. Material C lowered the mixing and compaction temperatures to a small extent.

#### **3.2.4 Linear viscoelastic behaviour**

Figures 9, 10, 11, 12 and 13 show the linear viscoelastic behaviour for the binders containing materials A to E compared to the neat 70/100 bitumen. These figures include the black diagram, temperature shift factors and the master curves of each binder based on the average of two replicate frequency sweeps.

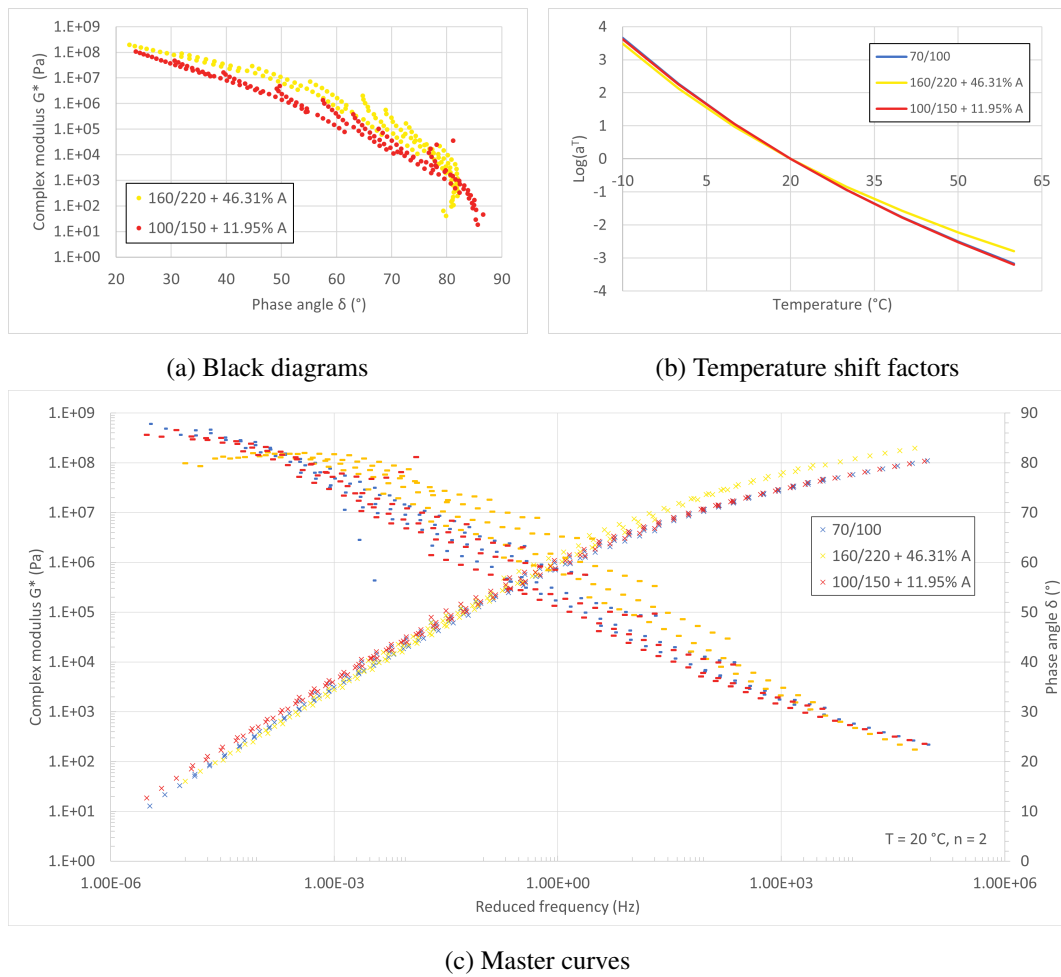


Figure 9: Linear viscoelastic behaviour material A

The continuous black diagrams in figure 9a of both binders containing material A allows the TTSP to be applied and master curves to be constructed. Furthermore, the black diagram for the 46.31% A binder indicated elastomeric behaviour, which corresponded with the increased elastic recovery as was observed in section 3.2.1. For the high concentration blend, the temperature shift factors in figure 9b showed decreased temperature dependency, which corresponded with the increased mixing and compaction temperatures observed in section 3.2.3 and increased rutting resistance in section 3.2.1. However, the low concentration blend also significantly increased mixing and compaction (Hz) temperatures and rutting resistance compared to the neat 70/100 bitumen, though the temperature shift factors were very similar. The master curve in figure 9c shows increased stiffness of the 11.95% A blend at low frequencies compared to the 70/100 bitumen, while the 46.31% A blend showed similar stiffness at low frequencies. It was expected that increased stiffness at low frequencies would result in worse fatigue resistance. However, in section 3.2.2, it was observed that the 11.95% A blend showed increased fatigue resistance in the TS, while the 46.31% A blend performed significantly worse. At high frequencies, the 11.95% A blend showed similar

stiffness to the 70/100 bitumen, while the 46.31% blend showed increased stiffness. The phase angle of the low concentration blend was very similar to the 70/100 bitumen for the whole frequency range. The high concentration blend showed a slightly elevated phase angle over the intermediate frequency range and lower at high frequency range.

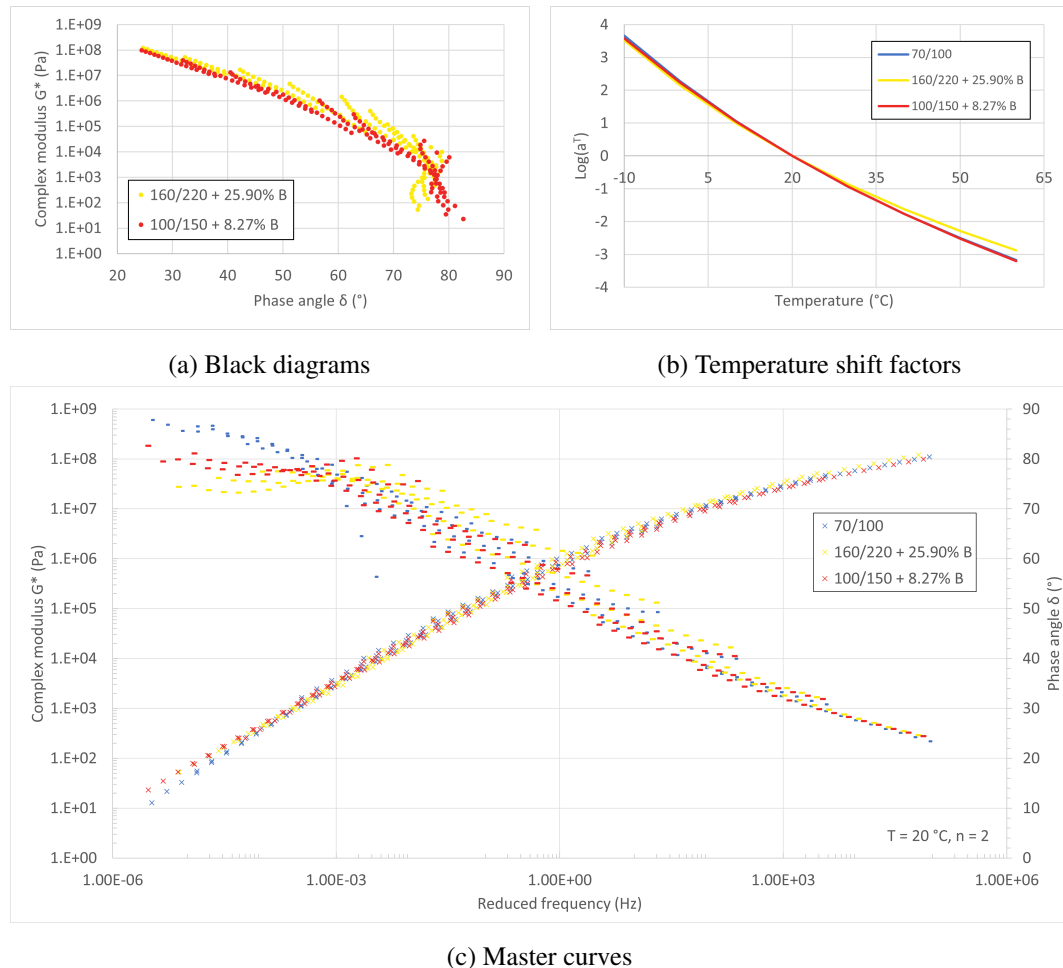


Figure 10: Linear viscoelastic behaviour material B

Figure 10a shows continuous black diagrams for both blends using material B, and thus allowed the formation of master curves. The black diagram for the 25.90% B binder seemed to indicate some elastomeric behaviour, as was seen in section 3.2.1. For the 8.27% B binder, no clear elastomeric behaviour could be identified from the black diagram, though this was observed in section 3.2.1. The temperature shift factors for the 8.27% B binder in figure 10b were very similar to the 70/100 bitumen, as were the mixing and compacting temperatures as observed in section 3.2.3. The increased rutting resistance of the 8.27% B binder as observed in section 3.2.1 was not reflected by the temperature dependency. The 25.90% B blend showed a significant temperature dependency reduction at higher temperatures, which corresponded with the increased mixing and compacting temperatures and increased rutting resistance. From the complex modulus  $G^*$  master curve in figure 10c, it was observed that

both blends showed increased stiffness at low frequencies compared to the 70/100 bitumen. In section 3.2.2, it was observed that the 25.90% B blend showed worse fatigue resistance while the 8.27% showed similar fatigue resistance to the 70/100 bitumen. The stiffness of both binders ranging from the intermediate to high frequency range was similar to the 70/100 bitumen, as was the phase angle. At low frequencies, the phase angle of the binders were observed to be lowered compared the 70/100 bitumen with the increase of material B in the binder.

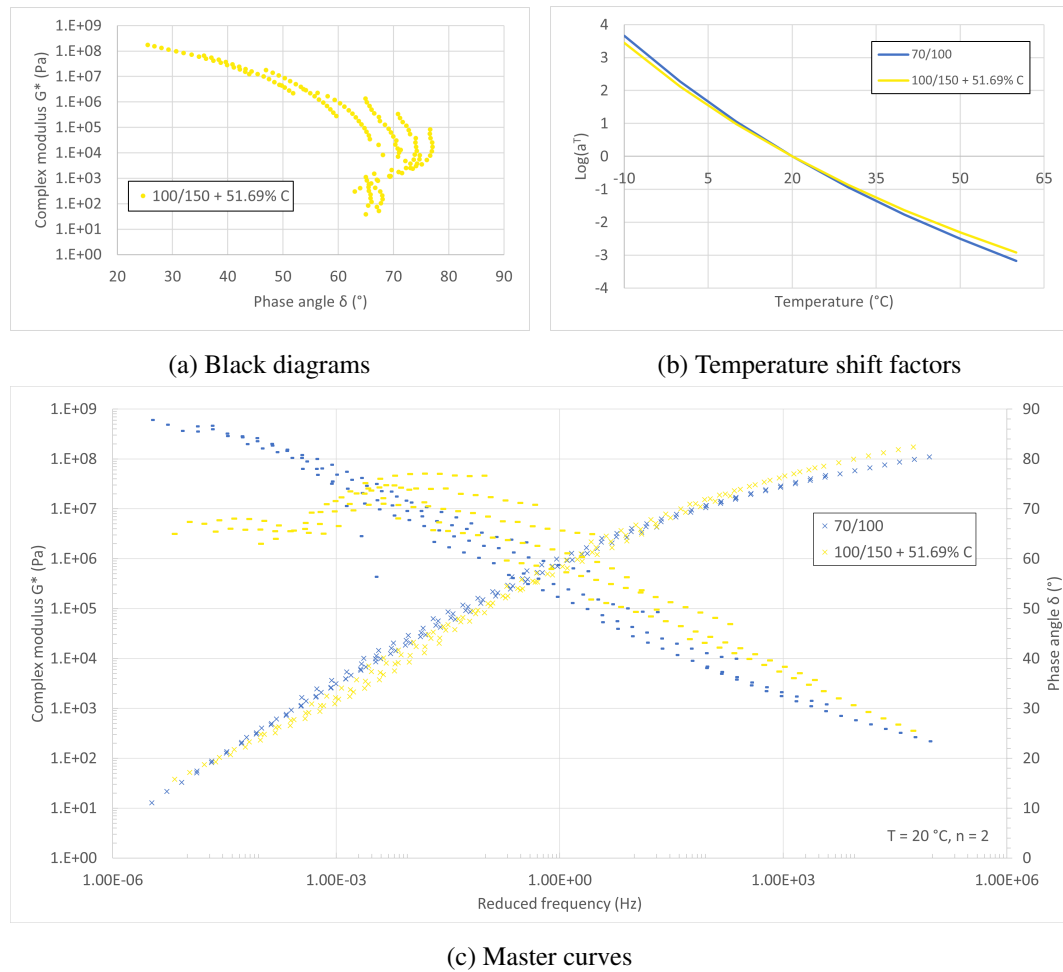
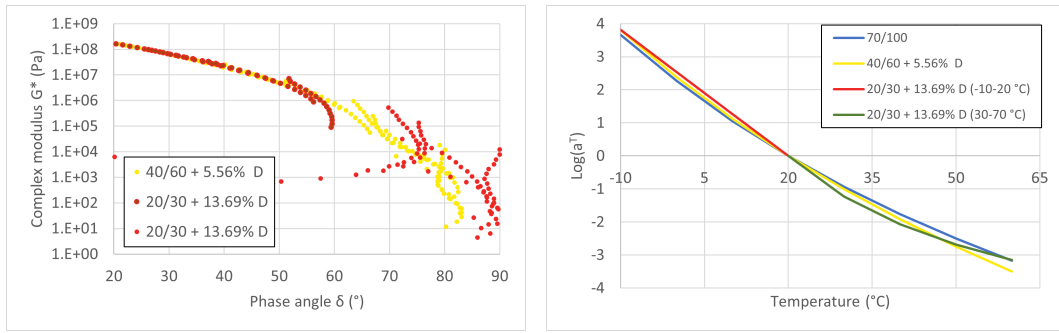


Figure 11: Linear viscoelastic behaviour material C

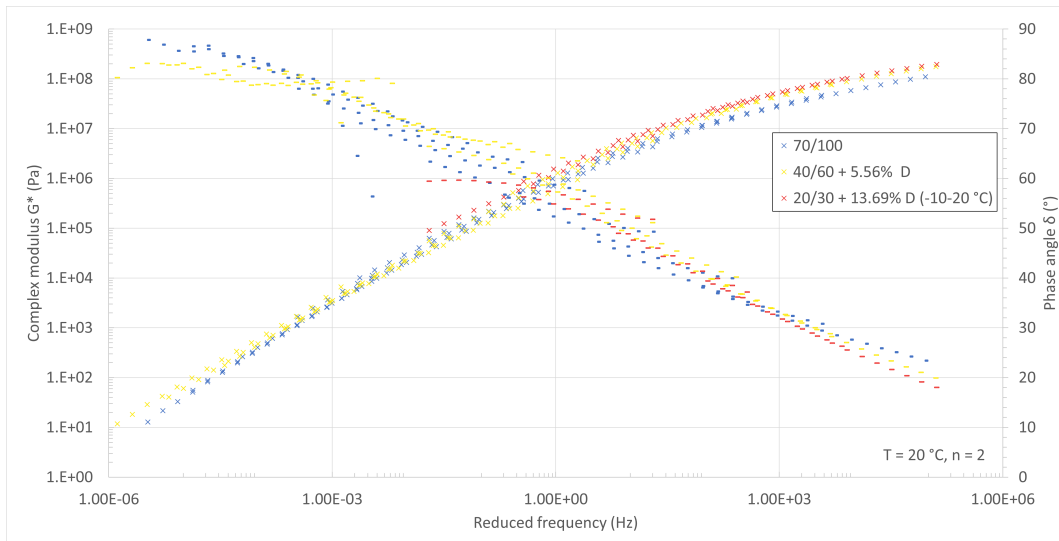
The continuous black diagram of the binder containing material C as observed in figure 11a allowed the application of the TTSP and the creation of a master curve. The high elastomeric behaviour indicated by the black diagram corresponded with the increased elastic recovery observed in section 3.2.1. Figure 11b shows decreased temperature dependency of the binder, while sections 3.2.3 and 3.2.1 showed significantly lower mixing and compaction temperatures and increased rutting resistance for the binder compared to the 70/100 bitumen respectively. The master curve in figure 11c shows slightly increased stiffness at low frequencies, but lower stiffness at low to intermediate stiffness compared to the 70/100 bitumen.

In section 3.2.2, it was observed that the binder containing material C showed significantly increased fatigue resistance compared to the 70/100 bitumen. At high frequencies the binder displayed a higher stiffness. From the phase angle master curve, it can be seen that the phase angle of the binder was elevated from the high to intermediate frequency range compared to the 70/100 bitumen. At low frequencies, the binder showed a significantly lower phase angle.

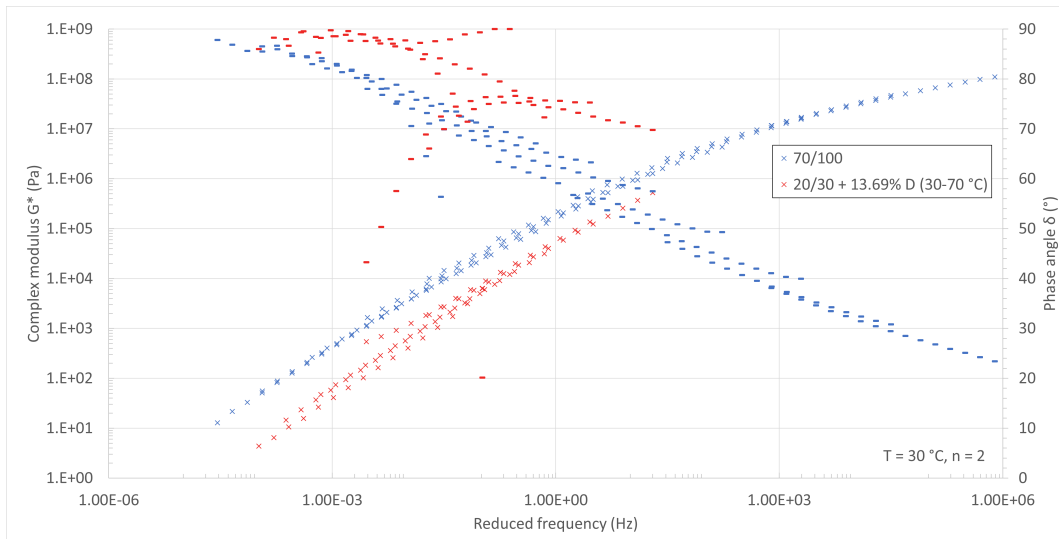


(a) Black diagrams

(b) Temperature shift factors



(c) Master curves (reference temperature = 20  $^\circ\text{C}$ )



(d) Master curves (reference temperature = 30  $^\circ\text{C}$ )

Figure 12: Linear viscoelastic behaviour material D

The linear viscoelastic behaviour of the binder containing 13.69% D resulted in a non-continuous black diagram, as seen in figure 12a. It was observed that there were in fact two different continuous black diagrams for the 13.69% D binder, being from -10 to 20 °C and 30 to 70 °C. For the 5.56% binder, no such effect was observed. The decreasing phase angle at low stiffnesses was not expected to be caused by elastomeric behaviour, but more due to the use of a low strain level in the frequency sweeps resulting in inaccurate measurements. The WLF equation was fitted to both the low and high temperature ranges separately for the 13.69% D binder using a reference temperature of 20 and 30 °C respectively. In figure 12b, the WLF function using a reference temperature of 30 °C was shifted to 20 °C to allow an easier comparison. Figure 12b shows increased temperature dependency for both binders containing material D, which corresponded with the lower mixing and compaction temperatures observed in section 3.2.3 and lower rutting resistance in section 3.2.1. Figure 12c shows increased stiffness of the 5.56% D binder at low frequencies compared to the 70/100 bitumen which corresponds with the decreased fatigue resistance as observed in section 3.2.2. In figure 12d, the 13.69% D binder shows softer behaviour at low frequencies compared to the 70/100 bitumen at a reference temperature of 30 °C, though section 3.2.2 showed decreased fatigue resistance for this binder. At high frequencies, both binders containing material D showed increased stiffness compared to the 70/100 bitumen. The phase angle master curves show similar behaviour of the binders compared to the 70/100 bitumen at the low to intermediate frequency range. At high frequencies, the 5.56% D binder showed a decreased phase angle, while the 13.69% D blend showed an increased phase angle at low frequencies at a reference temperature of 30 °C.

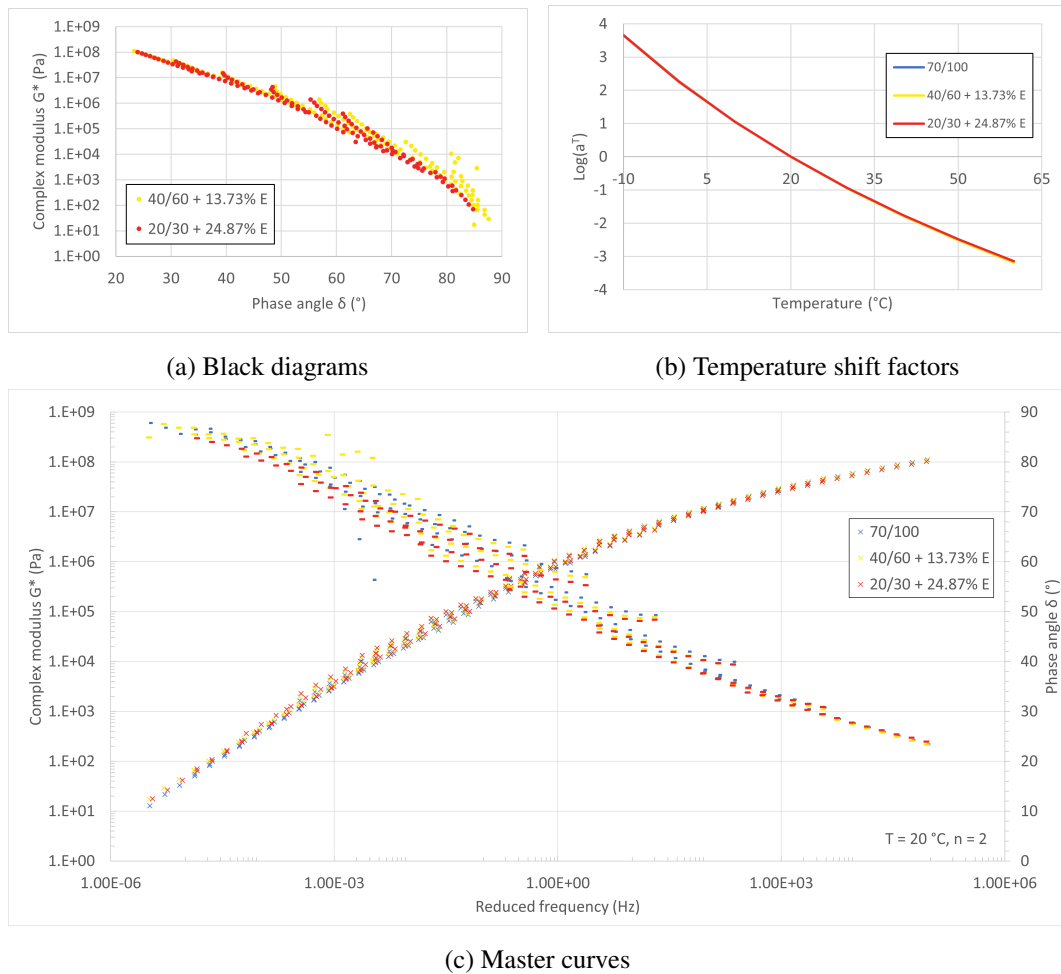


Figure 13: Linear viscoelastic behaviour material E

Overall, the linear viscoelastic behaviour of the blends containing material E showed very little difference to the 70/100 bitumen as seen in figure 13. The black diagrams of both blends were continuous, allowing the application of the TTSP. The black diagrams indicated no significant elastomeric behaviour, which agreed with section 3.2.1. From figure 13b, it can be observed that there was no significant difference between the blends and 70/100 bitumen for the temperature dependency. However, sections 3.2.3 and 3.2.1 showed slightly decreased mixing and compaction temperatures and slightly increased rutting resistance respectively. The master curves were also very similar for both the complex modulus and phase angle. From low to intermediate frequencies, both blends containing material E presented slightly stiffer behaviour compared to the 70/100 bitumen. From intermediate to high frequencies, both blends showed slightly softer behaviour. However, the 24.87% E blend showed increased fatigue resistance compared to the 70/100 bitumen in section 3.2.2. For the phase angle, no significant differences were observed.

### 3.2.5 Multi criteria analysis

To compare the overall performance of the binders, a Multi Criteria Analysis (MCA) was constructed based on the rutting and fatigue resistance, elastic recovery and mixing and compaction temperatures as criteria. For each criteria, the results were first normalized between 0 and 100 between the worst and best performing binder. The normalized scales were then shifted such that the neat 70/100 bitumen scored 0 on each criteria, where better performing binders scored higher than 0 and worse performing binders below 0. For the rutting resistance, the  $J_{nr}$  value at 0.1 kPa was taken, since this stress level correlates more to asphalt mixture rutting resistance than for 3.2 kPa [24]. For consistency,  $R$  was also taken at 0.1 kPa for the elastic recovery. For fatigue resistance, the average of the two TS at 5% strain were taken. For both mixing and compaction temperatures, the average of the two replicates were taken. In table 4, the results of the MCA are shown.

Blends	Rutting resistance	Elastic recovery	Fatigue resistance	Mixing temperature	Compaction temperature	Weighted average
<i>Weight</i>	<i>0.25</i>	<i>0.25</i>	<i>0.25</i>	<i>0.125</i>	<i>0.125</i>	
160/220 + 46.31% A	17.1	9.4	-15.5	-53.2	-55.5	-10.8
100/150 + 11.95% A	5.3	-0.9	1.8	-27.9	-24.1	-5.0
160/220 + 25.90% B	18.3	29.6	-16.8	-49.8	-39.8	-3.4
100/150 + 8.27% B	9.8	19.6	10.0	0.1	-1.0	9.7
100/150 + 51.69% C	17.2	66.5	82.1	14.8	22.5	46.1
40/60 + 5.56% D	-11.5	-3.1	-17.7	21.5	28.3	-1.8
20/30 + 13.69% D	-81.7	-33.5	-17.9	46.8	44.5	-21.9
40/60 + 13.73% E	2.3	-8.1	-1.6	-2.5	1.8	-1.9
20/30 + 24.87% E	7.2	-0.5	21.4	-0.7	-4.0	6.4
70/100	0.0	0.0	0.0	0.0	0.0	0.0

Table 4: Binder performance multi criteria analysis

In the MCA, the different performance indicators were equally weighted except for the mixing and compaction temperatures, since these are highly correlated. It is expected that some performance indicators, such as fatigue, are more important than others such as elastic recovery, however, determining the exact weights was not within the scope of this research. From table 4, it can be seen that only the 100/150 + 8.27% B, 100/150 + 51.69% C and 20/30 + 24.87% E blends outperform the neat 70/100 bitumen, while the other binders resulted in a negative weighted average. Still, the extent by which most binders underperformed compared to the 70/100 bitumen is marginal. This could change easily when some criteria were weighted differently, or criteria such as environmental impact were included in the MCA. Noteworthy is the great extent by which the 100/150 + 51.69% C binder outperformed the 70/100 bitumen while the 20/30 + 13.69% D binder significantly underperformed.

## 4 Conclusion

In this research, five circular materials were individually evaluated on their performance as bitumen substitute to serve as a mean for achieving an environmentally sustainable asphalt construction industry. From the results obtained, several conclusions can be drawn based on the performance of these circular materials in binders and the methods used, as listed below:

- Fatigue resistance of binders determined using VECD frameworks based on linear amplitude sweeps should always be validated using time sweeps. To determine the fatigue resistance of binders, a quicker more reliable method is to perform a single time sweep at a high but representative strain level such as 5% at a representative temperature.
- Binder performance does not always correlate with linear viscoelastic behaviour such as master curves. Performance tests such as time sweeps, multiple stress creep recovery and viscosity measurements should always be performed alongside when determining binder performance.
- Binders containing temperature susceptible circular materials require higher mixing and compaction temperatures than the temperature at which they are significantly negatively affected. Limiting the mixing and compaction temperature could result in the insufficient mixing and/or compaction of asphalt mixtures.
- Materials B, C and E are able to increase overall binder performance compared to neat bitumen for certain weight ratios, though this could potentially also apply to materials A and D depending on the considered performance criteria and their importance. Material C shows the greatest potential in increasing binder performance, whereas material D shows the least potential.
- The asphalt construction industry can increase binder performance by substituting bitumen by circular materials in binders for asphalt mixtures, in turn potentially lowering the environmental impact due to increased asphalt mixture performance and less need of bitumen.

## 5 Future work

Although the outcomes of the research work presented in this paper are already meritorious in 'paving the way' towards an environmentally sustainable asphalt construction industry, their reach, depth and validity might benefit from performing the following additional research activities:

- Asses the environmental sustainability of the circular materials as bitumen substitutes in asphalt mixtures by the means of an Life Cycle Assessment.
- Investigate measures to reduce the required mixing and compaction temperatures of binders containing temperature susceptible circular materials.
- Evaluate the susceptibility to aging of the circular materials as bitumen substitute on linear viscoelastic behaviour, rutting and fatigue resistance.
- Evaluate the performance of combined circular materials as 100% bitumen replacement.
- Evaluate the performance of the circular materials combined with aged bitumen from reclaimed asphalt.
- Validate the results of this study by performing stiffness, fatigue and rutting tests on asphalt mixtures including the circular materials as bitumen substitute.

## References

- [1] United Nations Framework Convention on Climate Change, "The Paris Agreement," 2021.
- [2] M. Allen, M. Babiker, Y. Chen, M. Taylor, P. Tschakert Australia, H. Waisman, R. Warren, P. Zhai, K. Zickfeld, P. Zhai, H.-o. Pörtner, D. Roberts, J. Skea, P. Shukla, A. Pirani, W. Moufouma-Okia, C. Péan, R. Pidcock, S. Connors, J. Matthews, Y. Chen, X. Zhou, M. Gomis, E. Lonnoy, T. Maycock, M. Tignor, and T. Waterfield, "Special Report 2018 IPCC: Summary for Policymakers," tech. rep., IPCC, 2018.
- [3] Manuel Kaal and Evelien Damhuis, "Hoe kijkt Nederland aan tegen het klimaat en klimaat-verandering?," tech. rep., Kantar, 2020.
- [4] Hoge Raad der Nederlanden, "Dutch State to reduce greenhouse gas emissions by 25% by the end of 2020," 12 2019.
- [5] Raad van State, "PAS mag niet als toestemmingsbasis voor activiteiten worden gebruikt," 4 2019.
- [6] Rechtbank Den Haag, "Royal Dutch Shell moet CO2-uitstoot terugbrengen," 5 2021.

- [7] Bouwend Nederland, “Onderbouwing TOP 25 duurzame opdrachtgevers,” tech. rep., Bouwend Nederland, Zoetermeer, 10 2020.
- [8] EAPA, “Asphalt in figures 2017,” tech. rep., EAPA, 2017.
- [9] L. Overmars, “LCA achtergrondrapport SBS en EVA gemodificeerd bitumen uit Europa t/m 10% modificatie, cat. 3,” tech. rep., Ecochain Technologies B.V., Amsterdam, 6 2020.
- [10] Z. Y. Mahssin, N. Abdul Hassan, H. Yaacob, M. H. Puteh, C. R. Ismail, R. Putra Jaya, M. Mohammad Zainol, and M. Z. Mahmud, “Converting Biomass into Bio-Asphalt - A Review,” in *IOP Conference Series: Earth and Environmental Science*, vol. 682, IOP Publishing Ltd, 2 2021.
- [11] M. Zahoor, S. Nizamuddin, S. Madapusi, and F. Giustozzi, “Recycling asphalt using waste bio-oil: A review of the production processes, properties and future perspectives,” 3 2021.
- [12] J. Bari, “Development of a New Revised Version of the Witczak E\* Predictive Models for Hot Mix Asphalt Mixtures,” tech. rep., Arizona State University, 2005.
- [13] V. Radhakrishnan, M. Ramya Sri, and K. Sudhakar Reddy, “Evaluation of asphalt binder rutting parameters,” *Construction and Building Materials*, vol. 173, pp. 298–307, 6 2018.
- [14] H. Liu, W. Zeiada, G. G. Al-Khateeb, A. Shanableh, and M. Samarai, “Use of the multiple stress creep recovery (MSCR) test to characterize the rutting potential of asphalt binders: A literature review,” *Construction and Building Materials*, vol. 269, 2 2021.
- [15] A. Subhy, “Advanced analytical techniques in fatigue and rutting related characterisations of modified bitumen: Literature review,” 12 2017.
- [16] F. Safaei, C. Castorena, and Y. R. Kim, “Linking asphalt binder fatigue to asphalt mixture fatigue performance using viscoelastic continuum damage modeling,” *Mechanics of Time-Dependent Materials*, vol. 20, pp. 299–323, 8 2016.
- [17] W. Cao and C. Wang, “A new comprehensive analysis framework for fatigue characterization of asphalt binder using the Linear Amplitude Sweep test,” *Construction and Building Materials*, vol. 171, pp. 1–12, 5 2018.
- [18] F. Safaei and C. Castorena, “Temperature effects of linear amplitude sweep testing and analysis,” *Transportation Research Record*, vol. 2574, pp. 92–100, 2016.
- [19] Y. Yildirim, M. Solaimanian, and T. W. Kennedy, “Mixing and compaction temperatures for hot mix asphalt concrete,” tech. rep., 2000.

- [20] G. D. Airey, "Use of Black Diagrams to Identify Inconsistencies in Rheological Data," *Road Materials and Pavement Design*, vol. 3, pp. 403–424, 1 2002.
- [21] N. Saboo and P. Kumar, "Equivalent Slope Method for Construction of Master Curves," tech. rep., 2018.
- [22] R. N. Hunter, A. Self, and J. Read, *The Shell Bitumen Handbook*, vol. 6. 2015.
- [23] C. Varanda, I. Portugal, J. Ribeiro, A. M. Silva, and C. M. Silva, "Optimization of bitumen formulations using mixture design of experiments (MDOE)," *Construction and Building Materials*, vol. 156, pp. 611–620, 12 2017.
- [24] K. Blazejowski and B. Dolzycki, "The relationships between asphalt mix rutting resistance and MSCR test results," tech. rep., 2014.